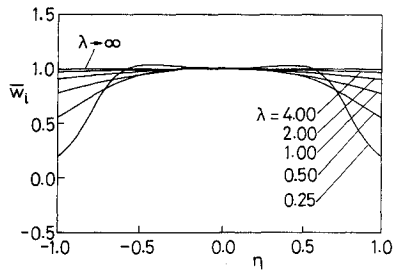

Fig. 2 Total downwash induced by the trailing vortex system over a range of values of λ for the elliptic loading $\bar{\Gamma}_1 = \sin\theta$. The downwash $\bar{w}_i$ has been normalized by $U_\infty A_1$. This value is equal to the constant downwash for the elliptic loading in Prandtl's classical theory for high aspect ratio wings.

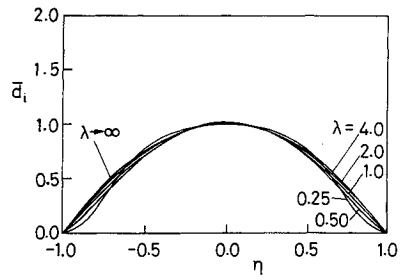

Fig. 3 Distribution of the induced drag. The drag components $\bar{d}_i$ have been normalized by $4\rho b^2 U_\infty^2 A_1^2$. This value is the least drag predicted by Prandtl's theory. The distribution of the least drag is also plotted for comparison.

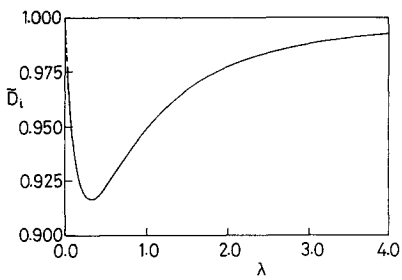

Fig. 4 Total induced drag as a function of the downstream distance λ, $\lambda_o = 0.33$.

tance. The progressive changes in the upwash toward the tips are particularly interesting for increasing values of λ. Prandtl's original results may be recovered as an asymptotic limit of the present model when the rolling-up process would have completed after a downstream distance of two wing spans. It is interesting to compare with the analytic results of Kaden[8] that the downstream distance x_r of complete roll up is given by $x_r/b \sim 0.56(A/C_L)$. This distance equals two and four spans for C_L being 1.0 and 0.5, respectively, for a wing of aspect ratio 7. The integrand of the induced drag $\bar{d}_i$ illustrates the distribution of the drag across the wing span as the parameter λ varies (Fig. 3). The variation in the drag distribution at lower values of λ is particularly noticeable, since the integrated values represent the measure of the induced drag. The vanishing drag at the wingtips is a direct result of the assumption of zero circulation at these points. The relation of the drag with the total lift is implicitly contained in the first coefficient A_1. Figure 4 shows one of the most important conclusions derived from the present study: For the loading case examined, there is an optimum downstream distance λ_o for completion of the rolling up, which results in a minimum induced drag meaningfully lower than the classical limit. Note that the unity indicates the classical value of the least drag. This potential energy picture immediately reminds us of the analogous potential of the interaction between atoms existing among the microscopic structure of matter. At short distance of λ, the downwash is dominant by the repulsive effect of the concentrated line vortices, whereas the attractive influence of the planar vortex sheet manifests itself at large distance of λ. The minimum drag attains when the effect of the concentrated line vortices is in an equilibrium state with the influence of the vortex sheet in the similar way as what happens in the achievement of the neutral position between repulsion and attraction among the atoms of matter.

Conclusions

An improved lifting-line theory for inviscid flow, taking into account some mean effect of trailing vortex sheet roll up with the downstream distance, has been developed. Calculations based on the wing wake model show that, for a given load distribution commonly encountered in practice, the roll up of the sheet within a downstream distance comparable to the wing span results in a reduced induced drag relative to the value evaluated by the classical lifting-line theory of Prandtl. This benefit comes from the variation in the downwash velocity field brought about by the rolled-up line vortices.

Acknowledgments

The present study is a part of the research on the possibility of induced drag reduction sponsored by British Aerospace plc. The author wishes to thank the Croucher Foundation and its Trustees for providing him a scholarship while this research work was being undertaken. Thanks also go to D. J. Maull and M. Gaster for their interest and useful discussions on this topic.

References

[1]Lanchester, F. W., *Aerodynamics,* Constable and Co., London, 1907.

[2]Fage, A., and Simmons, L. F. G., "An Investigation of the Airflow Pattern in the Wake of an Aerofoil of Finite Span," British Aeronautical Research Council, R&M 951, 1925.

[3]Prandtl, L., "Application of Modern Hydrodynamics to Aeronautics," NASA R-116, 1919.

[4]Batchelor, G. K., "Axial Flow in Trailing Line Vortices," *Journal of Fluid Mechanics,* Vol. 20, Pt. 4, 1964, pp. 645-658.

[5]Lam, F., "On the Induced Drag of Wings of Finite Aspect Ratio," Cambridge Univ. Engineering Dept. TR-17, 1991.

[6]Lamb, H., *Hydrodynamics,* Cambridge Univ. Press, 1932, Chap. VII.

[7]Glauert, H., *The Elements of Aerofoil and Airscrew Theory,* Cambridge Univ. Press, 1926, Chap. X and XI.

[8]Kaden, H., "Aufwickling einer Unstabilen Untetigkeitsfläche," *Ingenieur Archiv,* Bd 2, 1931, pp. 140-168.

Two-Equation Turbulence Model for Compressible Reacting Flows

J. R. Narayan*
NASA Ames Research Center,
Moffett Field, California 94035

Introduction

ONE of the major areas of current interest where computational fluid dynamics (CFD) is used extensively is the development of advanced air-breathing propulsion systems for hypersonic vehicles. A hydrogen-fueled supersonic combus-

Received Jan. 13, 1992; revision received July 9, 1992; accepted for publication July 10, 1992.

*Research Scientist, MCAT Institute. Member AIAA.

tion ramjet (scramjet) is such a propulsion system. The scramjet flowfield is highly complex. Interactions of several physical phenomena occur inside the combustor. The interaction between turbulent mixing process and combustion is of particular interest here. The extent and nature of these interactions partially dictate the size of the combustor to achieve the desired performance levels. An extensive study of this problem in a test facility is not possible at present due to the lack of such facilities. Fortunately, current CFD tools are able to address this crucial need to some extent. Their capabilities vary according to the extent to which detailed modeling of the various physical processes involved is carried out. The code SPARK[1] developed at NASA Langley Research Center is an example of such a prediction tool. The prediction method must be capable of addressing high-speed turbulent reacting compressible fluid flows involving high energy release. One major drawback of most of the prediction methods is that the turbulence-combustion interactions are not addressed adequately. These interactions are extremely difficult to model, which explains the dearth of reliable models. The present paper represents the initial effort at establishing a solution procedure for the computation of turbulent compressible reacting flows.

The Navier-Stokes equations (density weighted) along with equations for energy and species continuity that govern flows with multiple species undergoing chemical reaction have been used.[2] In spite of the advances made in the area of turbulence modeling in recent years, no universal model, applicable to complex flow problems such as described earlier, has emerged. The model should not only be accurate but also economical to use in conjunction with the governing equations of the fluid flow. Based on these considerations, a two-equation turbulence model has been chosen for the analysis.[2,3] The model solves differential equations for the turbulent kinetic energy and its dissipation rate. A compressibility correction model has been added to the turbulent kinetic energy equation.[4] A finite rate chemistry model[5] for a hydrogen-air reaction system has been used.

A major portion of the chemical reactions in the combustor occur in mixing layers that exist between fuel and airstreams. Mixing layers ranging from subsonic to supersonic speeds have been studied extensively over the years.[3,6,7] However, reliable experimental data for reacting mixing layers is limited. In the present work, mixing dominated flowfields (reacting and nonreacting) of axisymmetric and planar configurations have been computed. Available experimental data[8] are used to validate the model predictions.

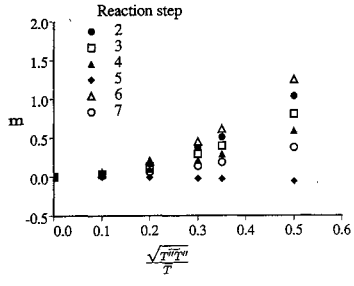

Fig. 1 Effect of temperature fluctuations on reaction rate.

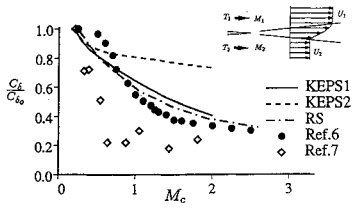

Fig. 2 Compressible mixing-layer growth rate.

Table 1 H_2-Air reaction system (7 steps)

Number	Reaction
1	$H_2+O_2 \rightarrow OH+OH$
2	$H+O_2 \rightarrow OH+O$
3	$OH+H_2 \rightarrow H_2O+H$
4	$O+H_2 \rightarrow OH+H$
5	$OH+OH \rightarrow H_2O+O$
6	$H+OH+M \rightarrow H_2O+M$
7	$H+H+M \rightarrow H_2+M$

The effect of compressibility is included as an additional turbulence energy dissipation rate[4] in the turbulent kinetic energy equation. This term is given by

$$\epsilon_c = \alpha M_t^2 \epsilon \tag{1}$$

Here, M_t the local turbulent Mach number defined as $M_t^2 = 2k/a^2$, where a is the local speed of sound and k the turbulent kinetic energy. The model constant $\alpha = 1.0$.

A differential equation for the variance of static enthalpy ($\widetilde{h''h''}$) has been included in the solutions. The modeled equation takes a form similar to that of the turbulent kinetic energy.[2] This equation is included to model the effect of temperature fluctuations on the species production rate. The Arrhenius reaction rate equation is written in terms of mean and fluctuating components of the temperature and expanded in a series. The terms are truncated at the second-order level, and the calculated variance of enthalpy is used to evaluate the resultant reaction rate term. The effect of turbulent fluctuations in species concentrations on the production rate is not included in the present work (this effort is underway).

The Arrhenius rate equation,

$$k_f = AT^b \exp\left[-\frac{T_a}{T}\right] \tag{2}$$

is written as

$$k_f = A(\tilde{T}+T'')^b \exp\left[-\frac{T_a}{(\tilde{T}+T'')}\right] \tag{3}$$

In Eqs. (2) and (3), T is the temperature, k_f the forward reaction rate, and A, b, and T_a are parameters associated with the rate term. Assuming that $T''/\tilde{T}<1$, the terms containing $(\tilde{T}+T'')$ can be expanded in a series, and the resultant modified reaction rate term is written as,

$$\widetilde{k_f} = (1+m)A\tilde{T}^b \exp\left[-\frac{T_a}{\tilde{T}}\right]$$
$$m = \left[(b-1)\left(\frac{b}{2}+\frac{T_a}{\tilde{T}}\right)+\frac{1}{2}\left(\frac{T_a}{\tilde{T}}\right)^2\right]\frac{\widetilde{T''T''}}{\tilde{T}^2} \tag{4}$$

where T_a is the activation temperature. Terms of order higher than 2 in $T''/\tilde{T}$ are neglected from the series expansion for want of appropriate models for these higher-order terms. Figure 1 shows the magnitude of m for various values of the temperature fluctuation for the H_2-Air reaction model (Table 1) at a local mean temperature of 2000 K. The maximum value of m for a temperature fluctuation of 30% mean temperature is approximately 0.6 for the reaction steps 2–7 (Table 1) and is approximately equal to 5.0 for the first reaction step (not shown).

Results and Discussion

A two-dimensional, high-speed mixing layer is considered in the initial part of this study. A schematic of this flow problem is given in Fig. 2. The two streams (air) are supersonic, whereas the convective Mach number M_c (Ref. 7) of the mixing layer ranges from subsonic to supersonic values. Figure 2 shows the

comparison between the predictions and representative experimental data.[6,7] Here, C_δ is defined as

$$C_\delta = \frac{d\delta}{dx}\frac{U_1+U_2}{U_1-U_2}$$

and C_{δ_0} is its value for incompressible flow. KEPS1 refers to the predictions with compressibility correction included, and KEPS2 refers to the predictions without the correction. RS refers to the Reynolds stress closure predictions.[9] The scatter among the experimental data is indicative of the nature of available data. The effect of compressibility on the mixing-layer growth rate is to reduce the growth rate with increasing convective Mach number. The two-equation model without the compressibility correction does not predict the reduced growth rate with increasing compressibility. However, the compressible two-equation model does predict this trend very well. The close comparison between the Reynolds stress closure and the k-ϵ model is important because for complicated flowfields, such as that in the scramjet combustor, the higher-order Reynolds stress closure may be very expensive to use. The predictions agree well with experiment within the scatter in the available data. It must be pointed out that there are other compressibility correction models, similar to the one used here, available today. However, a detailed comparison between such models is beyond the scope of this report.

Mixing between fuel and air and the ensuing chemical reaction is the main focus of study for a configuration such as the scramjet combustor. The presence of turbulence and its effect on the flowfield, especially the mixing aspect of it, is an important part of such studies. A representative mixing dominated reacting flow (hydrogen and air) is considered here. A seven-step, seven-species H_2-Air reaction model (Table 1) has been used for the finite rate chemistry system considered here.

The test case studied is the reacting coaxial jet problem (Figs. 3) for which the experimental data was obtained by Evans et al.[8] In the experiment, hydrogen at a temperature of 251 K was injected (Mach number = 2.0 and velocity = 2418 m/s) along the axis of a supersonic jet (Mach number 1.9, velocity = 1510 m/s) of vitiated air (temperature = 1495 K). The species mass fractions in the airstream are nitrogen = 0.478, oxygen = 0.241, and water = 0.281. The fuel injector has an inner diameter of 0.6525 cm and outer diameter of 0.9525 cm. The outer jet (air) diameter is 6.53 cm. The predicted centerline distribution of hydrogen and the profiles of the major species mass fractions (H_2, O_2, H_2O, N_2) at three axial locations are compared with experimental data in Figs. 3. In these figures, D is the fuel injector outer diameter. The predictions agree well with experiment in the region where the mixing effects dominate. The discrepancy between the predictions and experiment immediately downstream of the injector exit may be due to the fact that the conditions set at the inlet location (boundary condition for computations) in the calculations may not match the exact experimental conditions. These conditions are unknown and, hence, could not be used for the calculations. The predicted profiles of water vapor, which is an indication of the extent of reaction, agree reasonably well with the experiment. The location of the peak in the profile is farther into the airstream for the predictions than the experiment indicates. This may be because the interaction between turbulence and chemistry is not fully accounted for in the calculations. As mentioned earlier, the calculations account for only the effect of temperature fluctuations on the reaction rate. In addition, correlations of order higher than 2 were dropped from the model. Also, the experimental data itself may not be very accurate. Given that, the compressible turbulence model used here performs very well in predicting the turbulent reacting flow.

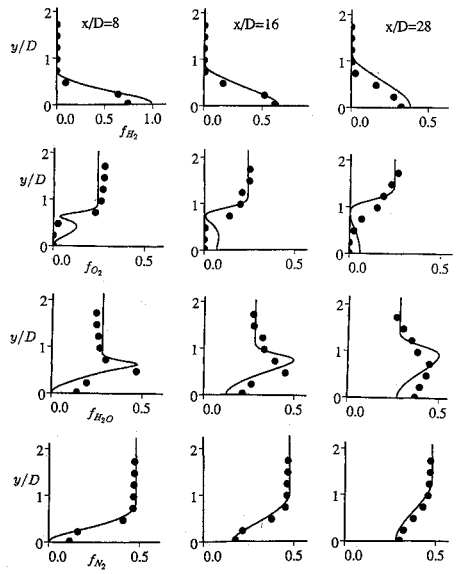

a) Species mass fractions H_2, O_2, H_2O, and N_2

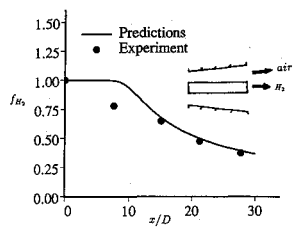

b) Centerline H_2 distribution

Fig. 3 Reacting flow: coaxial jets.

Conclusions

A two-equation turbulence model (k-ϵ) has been modified to be applicable for compressible flows by adapting a compressibility correction model. Computation of compressible mixing layers indicate that the decrease in the growth rate of the mixing layer with increasing convective Mach number is well predicted by the model. Comparisons of the predictions agree very well with available experimental data and the predictions of a compressible Reynolds stress closure. Preliminary studies of reacting mixing problems involving dissimilar gases indicate that the model is well suited for application to such flows. The computations use a model for the effect of temperature fluctuations on the reaction rate in the finite rate chemistry model. Further improvement to the model, especially the effect of turbulent fluctuations in species concentrations on the production rate, is necessary.

Acknowledgments

This work was supported by Theoretical Flow Physics Branch, Fluid Mechanics Division, NASA Langley Research Center under Contract NAS1-18599. The Technical Monitor was J. P. Drummond.

References

[1]Carpenter, M. H., "Three-Dimensional Computations of Cross-Flow Injection and Combustion in a Supersonic Flow," AIAA Paper 89-1870, June 1989.

[2]Narayan, J. R., "A Two-Equation Turbulence Model for Compressible Reacting Flows," AIAA Paper 91-0755, 29th Aerospace Sciences Meeting, Reno, NV, Jan. 1991.

[3]Narayan, J. R., and Sekar, B., "Computation of Turbulent High Speed Mixing Layers Using a Two-Equation Turbulence Model," *Proceedings of the CFD Symposium on Aeropropulsion,* NASA Lewis Research Center, Cleveland, OH, April 1990.

[4]Sarkar, S., Erlebacher, G., Hussaini, M. Y., and Kreiss, H. O., "The Analysis and Modeling of Dilatational Terms in Compressible Turbulence," NASA CR 181959, Dec. 1989.

[5]Jachimowski, C. J., "An Analytical Study of the Hydrogen-Air Reaction Mechanism with Application to Scramjet Combustion," NASA TP 2791, 1988.

[6]Birch, S. F., and Eggers, J. M., "A Critical Review of the Experimental Data for Developed Free Turbulent Shear Layers," NASA SP-321, 1973, pp 11-40.

[7]Papamoschou, D., and Roshko, A., "The Compressible Turbulent Shear Layer: An Experimental Study," *Journal of Fluid Mechanics*, Vol. 197, 1988, pp 453-477.

[8]Evans, J. S., Schexnayder, C. J., and Beach, H. L., "Application of a Two-Dimensional Parabolic Computer Program to Prediction of Turbulent Reacting Flows," NASA TP-1169, 1978.

[9]Sarkar, S., and Balakrishnan, L., "Application of a Reynolds Stress Turbulence Model to the Compressible Shear Layer," Inst. for Computer Applications in Science and Engineering, Rept. 90-18, Hampton, VA, Feb. 1990.

Improved Boundary Integral Method for Inviscid Boundary Condition Applications

P. Koumoutsakos* and A. Leonard†
California Institute of Technology, Pasadena, California 91125

I. Introduction

THIS Note deals with the computation of the potential part of an unsteady, incompressible, viscous flow around an arbitrary configuration and the enforcement of the no-through flow boundary condition. To solve the full problem, it should be complemented by a solver to account for the convective and viscous part of the flow.

To generate the velocity potential, one often uses boundary integrals. The boundary may be considered as a surface of discontinuity[1] (vortex sheet) and is usually discretized with panels. The inviscid boundary condition (no through flow) is then applied in a Neumann or Dirichlet form on the stream-function to determine the unknown vorticity distribution. However, the solution to this problem is not unique, and the additional constraint, of conservation of total circulation needs to be imposed. The resulting sets of equations are not numerically well-conditioned, and the accuracy of the solution deteriorates as the thickness of the body is decreased and/or the number of the panels increases. Here a rigorous approach is presented (similar to the one used in Ref. 2) involving the application of the internal Neumann boundary condition, in which the resulting system of equations is well-conditioned, thus permitting an efficient and accurate solution with direct or iterative matrix inversion techniques. The method does not increase the computational cost, and it is found to improve the conditioning of the system by several orders of magnitude, the improvement being more pronounced as the number of panels increases.

II. Governing Equations and Boundary Conditions

Consider a two-dimensional body, (s, n), in an incompressible viscous flowfield induced by a uniform flow and vorticity in the wake. The flow is governed by the Navier-Stokes equations, which may be expressed in terms of the vorticity ($\omega \hat{e}_z = \nabla \times u$) as:

$$\frac{\partial \omega}{\partial t} + u \cdot \frac{\partial \omega}{\partial x} = \nu \nabla^2 \omega \tag{1}$$

Received March 25, 1991; revision received April 17, 1992; accepted for publication April 22, 1992.

*Research Assistant, Graduate Aeronautical Laboratories.
†Professor of Aeronautics, Graduate Aeronautical Laboratories.

along with the continuity equation ($\nabla \cdot u = 0$) and the no-slip boundary condition on the body. Using now the continuity equation along with the definition of the vorticity, the velocity u may be determined by the solution of

$$\nabla^2 u = -\nabla \times \omega \hat{e}_z$$

or in terms of the stream function

$$\nabla^2 \Psi = \omega \tag{2}$$

with $u = \nabla \times \Psi \hat{e}_z$. The stream function may be decomposed as

$$\Psi = \Psi_0 + \Psi_{\text{ext}}$$

where Ψ_{ext} is a particular solution of Eq. (2) and may be computed via the Biot-Savart law and Ψ_0 is the solution of the respective homogeneous equation and is chosen so that the velocity satisfies the kinematic boundary condition of no-through flow on the body (or $\Psi = \text{const}$). Once the velocity field has been calculated, then Eq. (1) needs to be solved to obtain the full solution of the problem. A number of numerical methods (finite differences, vortex methods, spectral methods) may be employed, but this analysis is beyond the scope of this Note.

Here we present an efficient scheme to solve for the potential part of the flow, namely the solution of

$$\nabla^2 \Psi_0 = 0$$

with $\Psi_0 + \Psi_{\text{ext}} = \text{const}$ on the body.

We consider Ψ_0 to arise because of a vortex sheet along the boundary of the body so that the flowfield at any point x in the domain is described by the stream function

$$\Psi(x) = -\frac{1}{2\pi} \oint \log|x - x(s')| \frac{d\Gamma}{ds'} ds' + \Psi_{\text{ext}}(x) \tag{3}$$

where the stream function $\Psi_{\text{ext}}(x)$ includes the contribution from the freestream and the vorticity in the wake and $d\Gamma/ds$ denotes the circulation distribution of the vortex sheet. Applying the inviscid boundary condition and the additional constraint that the total circulation ejected from the surface of the nonrotating body is zero, respectively, results in Eqs. (4) and (5) for the Dirichlet and internal Neumann boundary conditions:

$$c = -\frac{1}{2\pi} \oint \log|x(s) - x(s')| \frac{d\Gamma}{ds'} ds' + \Psi_{\text{ext}}[x(s)] \tag{4a}$$

$$\oint \frac{d\Gamma}{ds'} ds' + \Gamma_{\text{wake}} = 0 \tag{4b}$$

and

$$\frac{d\Gamma}{ds} - \frac{1}{\pi} \oint \frac{\partial}{\partial n} [\log|x(s) - x(s')|] \frac{d\Gamma}{ds'} ds' = -2 \frac{\partial \Psi_{\text{ext}}}{\partial n} [x(s)] \tag{5a}$$

$$\oint \frac{d\Gamma}{ds'} ds' + \Gamma_{\text{wake}} = 0 \tag{5b}$$

These sets of equations may be solved to any accuracy by a panel method.[3] Discretizing the body with M vortex panels results in a system of equations for the M unknown strengths. The two linear sets of equations may be expressed in matrix form:

$Kf = g$ (Dirichlet boundary condition)

$Gf = h$ (Neumann boundary condition)